AFRL-SA-WP-TR-2017-0019

Developing Reliable Telemedicine Platforms with Unreliable and Limited Communication Bandwidth

Peter F. Hu, PhD; Shiming Yang, PhD

University of Maryland

October 2017

Final Report
for June 2016 to September 2017

Air Force Research Laboratory
711th Human Performance Wing
U.S. Air Force School of Aerospace Medicine
Aeromedical Research Department
2510 Fifth St., Bldg. 840
Wright-Patterson AFB, OH 45433-7913

NOTICE AND SIGNATURE PAGE

REPORT DOCUMENTATION PAGE

1. REPORT DATE *(DD-MM-YYYY)* 25 Oct 2017	2. REPORT TYPE Final Technical Report	3. DATES COVERED *(From – To)*

4. TITLE AND SUBTITLE Developing Reliable Telemedicine Platforms with Unreliable and Limited Communication Bandwidth	5a. CONTRACT NUMBER FA8650-16-2-6H08
	5b. GRANT NUMBER
	5c. PROGRAM ELEMENT NUMBER
6. AUTHOR(S) Peter F. Hu, Shiming Yang	5d. PROJECT NUMBER
	5e. TASK NUMBER
	5f. WORK UNIT NUMBER

7. PERFORMING ORGANIZATION NAME(S) AND ADDRESS(ES) University of Maryland, Baltimore 22 S. Greene St. R. Adams Cowley Shock Trauma Center, T5R46 Baltimore, MD 21201	8. PERFORMING ORGANIZATION REPORT NUMBER

9. SPONSORING / MONITORING AGENCY NAME(S) AND ADDRESS(ES) USAF School of Aerospace Medicine Aeromedical Research Dept/FHE 2510 Fifth St., Bldg. 840 Wright-Patterson AFB, OH 45433-7913	10. SPONSORING/MONITOR'S ACRONYM(S)
	11. SPONSOR/MONITOR'S REPORT NUMBER(S) AFRL-SA-WP-TR-2017-0019

12. DISTRIBUTION / AVAILABILITY STATEMENT

DISTRIBUTION STATEMENT A. Approved for public release. Distribution is unlimited.

13. SUPPLEMENTARY NOTES
Cleared, 88PA, Case # 2017-5936, 24 Nov 2017.

14. ABSTRACT
Telemedicine techniques could deliver health care services to battlefields and expedite, optimize patient care and triage. However, the communication networks in such environments are often unreliable and have limited bandwidth. In this study, we evaluated the accuracy loss and clinical decision error caused by data transmission. We compared physiologic data under various resampling rates with the original high-resolution data and reported the matrix to detailed trade-off between clinical accuracy and band resource requirement. Using data collected from 15,000 trauma patients, we found that heart rate readings could be within a 10% difference when reducing sampling rate from 2 seconds to 5 minutes. Moreover, the high-fidelity waveform could be reduced for sampling rate with a small (<5%) loss in prediction performance. This study could guide optimal selection of data sampling rate and estimation of data reliability based on the wireless bandwidth availability and acceptable vital signs resolution during the remote clinical decision making process.

15. SUBJECT TERMS
Telemedicine, physiologic data, communication

16. SECURITY CLASSIFICATION OF:			17. LIMITATION OF ABSTRACT	18. NUMBER OF PAGES	19a. NAME OF RESPONSIBLE PERSON Col Nicole Armitage
a. REPORT U	b. ABSTRACT U	c. THIS PAGE U	SAR	23	19b. TELEPHONE NUMBER *(include area code)*

This page intentionally left blank.

TABLE OF CONTENTS

LIST OF FIGURES

LIST OF TABLES

ii

1.0 SUMMARY

Telemedicine techniques could deliver health care services to battlefields or remote areas after a natural disaster. As a part of clinical decision support, physiologic data need to be transmitted to provide situational awareness for optimal patient care and triage. However, we often are faced with the challenge of limited bandwidth within these far forward and hostile environments. It is important to evaluate the accuracy loss and clinical decision error caused by data transmission in such environments. In this study, we precisely compared physiologic data under various resampling rates with the original high-resolution data and reported the matrix to detailed trade-off between clinical accuracy and band resource requirement. Using a large-scale dataset (15,000 cases) collected from real trauma patients, statistical attributes of physiologic data and their performance in some predictive models were compared in various simulated data downsampling rates. The results provide guidance for telemedicine network bandwidth selection, as well as design of future sampling schemes.

2.0 INTRODUCTION

In battlefields or remote areas after natural disaster, ad hoc networks are often used to establish temporary communication. Timely collected information from there allows less staff to be sent to the frontline and hence reduces risk and cost. It is important to guarantee the most important information could be transmitted when the bandwidth is limited. Although modern data compression techniques could be part of the solution, in this study we focused on the effect of data reduction on data statistical attributes. In this way, we could reduce the amount of data collection before doing compression while keeping the important statistics.

Typically, mean, minimum, maximum, quartiles, etc. are statistic quantities to summarize physiologic data in a given time window. Clinicians often use those quantities during the decision process. In this study, we considered heart rate (HR); non-invasive systolic blood pressure (NBPS), mean blood pressure (NBPM), and diastolic blood pressure (NBPD); respiratory rate (RESP); oxygen saturation (SpO2); temperature (TMP); and carbon dioxide (CO_2). From the raw data (1 data point every 2 seconds), we down sampled the data trajectories and compared the discrepancy.

Moreover, we analyzed the waveforms, which are collected at a much higher rate, e.g., 240 Hz. Waveform data are gaining popularity in clinical diagnosis and have been shown to be more useful in early prediction of some life-saving interventions (LSIs). It is important to reduce the amount of waveform transmissions while keeping the key statistical attributes. We tackled this problem using two approaches. In one approach we compared the key values derived from waveforms. For example, HR is often derived from electrocardiogram (ECG) waveforms by calculating the averaged peak-to-peak distances. The difference of estimated HR from waveforms of reduced sampling rates could help to find the optimal sampling data amount. In the second approach we tested the sampled data for some specific diagnosis/prediction, such as mortality, blood transfusion, or any other outcomes that could support urgent decision making. Using the sampled waveform as input for some prediction models and comparing the models' performance, we were able to directly examine the practical usefulness of downsampled waveform data.

1

3.0 BACKGROUND

The volume of real-time physiologic data has proliferated with advances in medical sensor technology. High-fidelity data are streamed into physiologic monitors for care planning, clinical decision support, and quality improvement. Such high throughput clinical data sensing and analyzing techniques are considered the future way to develop combat casualty autonomous resuscitation [1,2] and enhance real-time field decision making [3]. Many new monitoring indices or prediction models have been studied and developed based on those types of data, such as ECG, photoplethysmography (PPG), capnography, etc. Continuous non-invasive ECG and PPG sensors are ubiquitous in both prehospital emergency medical service and in-hospital health care for traumatic brain injury (TBI) patients. Waveforms measured from both sensors capture rich information of the cardiovascular, circulatory, and respiratory systems. Heart rate variability (HRV), derived from the ECG waveform, has long been used in studies of prehospital LSIs [4], neurologic disorders [5,6], and complications following severe TBI [7]. The association between HRV and autonomic nervous system and cardiovascular mortality is well established [8]. The autonomic nervous system is a complex life-sustaining system that plays a role in nearly every organ and disease [9], including regulating cardiac activity, respiration, and pupillary response. The PPG waveform has also been intensively studied due to the rich physiologic information it carries, such as HR, SpO2, and even RESP. Some novel models for diagnosing hemorrhagic shock [10] have been developed from the PPG waveform.

Although non-invasive and non-expensive medical sensors are becoming ubiquitous in emergency medical service and hospital health care, the benefit of high-resolution medical data is greatly limited in battlefield or natural disaster areas, where communication to remote medical facilities is restricted. In remote expeditionary care, challenges still exist when collecting and transmitting high-fidelity data. Specifically, these challenges include:

1. Limited resources during the expeditionary care phase in the hostile environment with longer term field care required in the expected anti-access/area denial environment in future conflicts followed by limited resources in the aeromedical evacuation environment. Telemedicine will be one way to provide extended care support and better prepare the receiving role II and III care teams.

2. To adequately support a future wireless deployment of the defense telemedicine communication network, we need to address the challenges of developing a reliable telemedicine platform with unreliable and limited communication bandwidth. To accomplish this goal, we must answer the following questions:

   a. What are the most critical patient vital features, incidents, or snippets to prioritize and transmit in a limited bandwidth environment to both maximize patient care and information for transport triage?
   b. What are the critical features of physiologic monitoring data that would convey the most useful information when transmitted?
   c. Can we adapt our previously developed algorithms dependent on continuous physiological data to utilize reduced vital signs (VS) resolution with similar predictive accuracy to optimize them for use in a low power and bandwidth environment?

2

d. How much effect does reduced VS resolution have on outcome prediction utilizing our previously developed algorithms developed for continuous data?

To investigate these questions, we developed a telemedicine bandwidth and VS feature matrix. This matrix provides specific VS critical feature changes with respect to reduced sampling rates and their associated bandwidth, e.g., the predictive value of mean systolic blood pressure changes as the sampling rate is changed from every 2 seconds to every 6 seconds, 30 seconds, 60 minutes, etc. To further study the effect of bandwidth-limited VS resolution and its associated outcome prediction power, we compared the accuracy of our current prediction algorithms based on the full-resolution and resampled VS waveforms, trends, and features.

We also compared the utility of full-resolution to reduced-resolution algorithms in real time in an adaptive analysis platform capable of analyzing individual or combining available inputs for the most accurate predictions possible. In previous U.S. Air Force funded studies, (FA8650-11-2-6D01 and FA8650-13-2-6D11), we explored the development of real-time thresholds, indices, and algorithms for clinical decision making. The algorithms utilizing demographics, single point field or admission VS, and high-quality continuous physiologic monitoring data including VS, ECG waveforms, and/or PPG waveforms for the prediction of the need for blood product transfusions and other LSIs in severely injured trauma patients. Those predictive models can be used as the evaluation tools of signals transmitted from a limited bandwidth network. The outcomes include blood transfusion needs, mortality, and hospital length of stay (LOS), which are critical for decision making in the battlefield.

The overall aim of this study was to determine the optimal features of a telemedicine platform that transfers the maximum amount of patient real-time data and information with the most conservative bandwidth and power requirements. This platform could be used for mass casualty awareness, improved patient care, and triage determinations for aeromedical evacuation in far forward or natural disaster scenarios with unreliable and limited communications bandwidth. The platform of adoptive algorithms will consider the available bandwidth and select the optimal VS and its resolution for data transfer to support the best outcome evaluation/prediction needs at the receiving location.

Our study tested the hypothesis that with a combination of limited VS resolution (bandwidth) and its associated features, we will be able to achieve acceptable outcome prediction (area under the receiver operating characteristic curve (AUROC)>0.8) and support remote patient triage and evaluation. Specifically, the following aims and tasks were included.

Aim 1: Develop a VS feature matrix that determines the most critical VS features that provide maximal information at each downsampling rate.

Task 1: Develop a high-resolution trauma patient resuscitation VS and outcome database for support of this study. Over the last 7 years (2009-2015), we have prospectively collected patient high-resolution VS during the first hour of trauma resuscitation at the University of Maryland R Adams Cowley Shock Trauma Center. We will merge a continuous physiological database of approximately 15,000 patients with the Trauma Registry to associate patient demographics and outcomes (emergency blood transfusion in 4, 12, 24 hours, mortality, LOS, length of intensive care unit stay) with the continuous physiological data.

Task 2: Develop the bandwidth optimization matrix described above.

3

Aim 2: Compare the accuracy of predictive algorithms using limited to full VS resolution. Utilize the outcome prediction power at different VS resolution to address the question of how much effect does reduced VS resolution have on outcome prediction and to identify the optimal sampling rate with the greatest degree of accuracy and requiring the least amount of bandwidth and/or power utilization. We adapt our previously developed algorithms dependent on continuous physiological data to utilize reduced VS resolution with similar predictive accuracy to optimize them for use in a low power and bandwidth environment

Task 3: Compare the predictive ability of our previously developed prediction algorithms results based on the original and resampled VS waveforms, trends, and the features calculated from the VS trends and waveforms.

Task 4: Compare the utility of a range of reduced-resolution to full-resolution predictive algorithms in real time in an adaptive analysis platform capable of analyzing individually or combining available inputs (ECG waveforms, pulse oximetry waveforms) to provide the most accurate predictions possible utilizing the least amount of data and/or bandwidth. This will be accomplished through simultaneous use of multiple algorithms associated with pulse oximetry and ECG signals (waveforms and numeric data) from the point of first encounter with the casualty, using both time-based analyses of the features.

4.0 METHODS

In the R Adams Cowley Shock Trauma Center, a level I regional trauma center located in downtown Baltimore, Maryland, 94 GE-Marquette-Solar-7000/8000® (General Electric, Fairfield, CT) patient VS monitors are networked to provide collection of real-time patient VS data streams in 13 trauma resuscitation unit (TRU), 9 operating room, 12 post-anesthesia care unit, and 60 intensive care unit individual bed/monitor units. Each patient monitor collects real-time 240-Hz waveforms and 0.5-Hz trends data that are transferred via secure intranet to a dedicated BedMaster® server (Excel Medical Electronics, Jupiter, FL) and archived [11]. This process generates approximately 20 million data points/day/bed or roughly 30 terabits/year of data. Physiological data collected through this system, when they are displayed on the GE Marquette monitor, include ECG, PPG, CO_2, arterial blood pressure, and intracranial pressure, among others. Trends include HR, RESP, TMP, end-tidal CO_2, and intracranial pressure, among many others. They cover the categories of brain pressure, cardiac, perfusion, and respiratory.

4.1 Case Selection and Sampling Method

In developing a VS feature matrix that determines the most critical VS features that provide maximal information at each downsampling rate, we created a matrix that shows feature changes with respect to reduced sampling rates. Focusing on the first hour of data, we selected 15,000 cases, with each case having satisfied two filters. The first filter removed individual data points that clinicians considered to be an extreme value. The second filter discarded cases that have fewer than 20 minutes of VS present in the first hour. We focused on the first hour because our prediction algorithm requires the first 15 minutes of data, up to 1 hour of data. These data are collected immediately after the patient is admitted to the TRU.

4

4.2 Trend Data Method

After 15,000 cases were selected, we downsampled them at seven different rates: 6 seconds, 30 seconds, 1 minute, 5 minutes, 10 minutes, 15 minutes, and 30 minutes. The raw trend data were sampled at 0.5 Hz, resulting in a data point every 2 seconds. For each downsampling rate, we compared the median of a given window to the first available value in the same window. For clarity, window size will refer to the number of points in a window; concurrently, sampling rate will refer to the length of time passed in each window. For example, when downsampling at a rate of 6 seconds, we looked at a window containing three values and calculated the median. We then compared the median to the first available value in the window. We repeated for each sampling rate on each variable for each case.

For a sampling rate of 6 seconds, 30 seconds, and 1 minute, each window requires all the data points, gapless. For 5, 10, 15, and 30 minutes, each window must contain at least 33% of the data. For example, a 150-point window (5 minutes) need only contain 50 points of data. Table 1 summarizes the data reduction ratios and bandwidth requirement for each downsampling rate. Gaps in data collection are a result of patients being transported between the TRU and the operating room receiving specialized scans or procedures.

Table 1. Data Reduction Ratios and Amount for Each Downsampling Rate for Trend and Waveform Data

Sampling Rate	Data Reduction Ratio	Trend (bps)	Wavelength (kpbs)
2 s (0.50 Hz)	1:1	160	40
6 s (0.17 Hz)	1:3	53	14
30 s (0.03 Hz)	1:15	11	2.66
1 min (0.02 Hz)	1:30	5	1.33
5 min (0.003 Hz)	1:150	3	0.266
10 min (0.002 Hz)	1: 300	1	0.133
15 min (0.001 Hz)	1:450	<1	0.088
30 min (0.0005 Hz)	1:900	<1	0.044

bps = bit per second; kbps = kilobit per second.

4.3 Waveform Method

Modern hospitals are often equipped with bedside monitors collecting various physiological data in a real-time, continuous, and automated way. Data ranging from routine intermittent observations to high-fidelity waveforms can be recorded and streamed into monitors for care planning, clinical decision support. Many new monitoring indices or prediction models have been studied and developed based on those types of data, such as ECG, PPG, capnography, and so on. Continuous non-invasive ECG and PPG sensors are ubiquitous in both prehospital emergency medical service and in-hospital health care for TBI patients. Waveforms measured from both sensors capture rich information of cardiovascular, circulatory, and respiratory systems. HRV, derived from ECG waveforms, has long been used in studies of prehospital LSIs, neurologic disorders, and complications following severe TBI.

5

However, high-fidelity waveform data create greater network traffic. It is necessary to evaluate the effect of sampling rates on the waveform data, especially on the performance of prediction models. We used a set of prediction models to evaluate the effect of various sampling rates. This set of prediction models included predicting uncrossmatched blood (UnX) use, massive transfusion (MT), critical administrative threshold (CAT), mortality, and LOS.

We collected data from 15,000 trauma patients from 2013 to 2015. The first 15 minutes ECG and PPG data after admission were used. The original sampling rate was 240 Hz. HRV variables were derived from both signals. To find QRS-peaks from ECG, the Pan Tompkins method was used [12]. The R-peaks were then detected based on a threshold that was adaptive to the signal. To detect PPG signal peaks and valleys, the Savitzky-Golay filter was applied to smooth the signal [13]. The peaks were found through two rounds of searching. In the first round, the peaks were roughly found through the Matlab imbedded software routine "findpeaks." The median distance between two consecutive peaks PD_{median} was then calculated. In the second round, any small peaks within a range of 0.6 x PD_{median} from a large peak were ignored. Figure 1 illustrates the peaks and valleys found for ECG and PPG signals. The normal-to-normal interval is the time interval between two consecutive R-peaks. HRV variables in time domain and nonlinear dynamics can be calculated based on the Task Force of the European Society of Cardiology and the North American Society of Pacing and Electrophysiology [8].
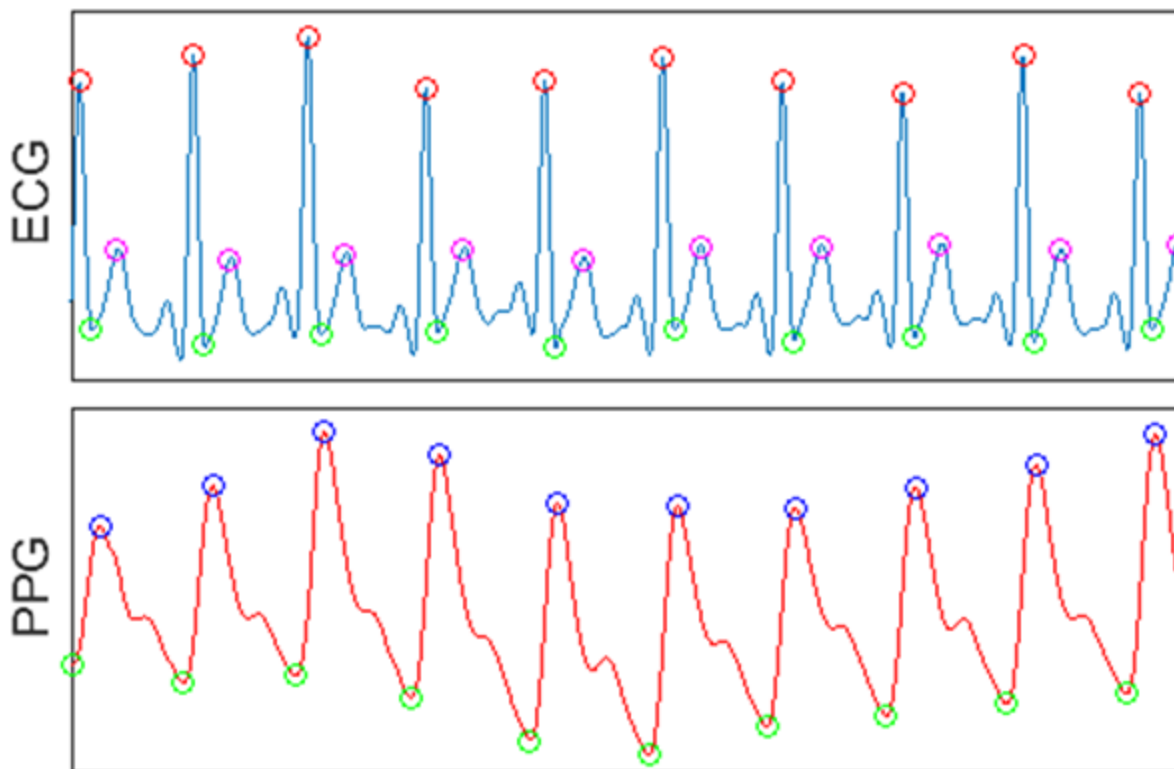

Figure 1. Peaks and valleys found for ECG and PPG waveforms.

6

Because signals may have been collected when the patient went through resuscitation, or had significant movement, artifacts exist and do not reflect the patient's real physiological status. To flag out signals with large amounts of artifact, signal quality can be evaluated based on R-peaks in ECG and the peaks in PPG. The assumption is that signal quality signals have normal distributed R-R intervals. R-R intervals from segments of low quality are detected as outliers using the Z-test.

PPG waveform-based variability and waveform morphology features can also be designed similarly with expansion based on PPG unique characteristics. From the PPG waveform, we extracted peak-to-peak time intervals, which are analog to the normal-to-normal intervals in ECG. PPG waveform-based variability and morphology features were calculated. PPG waveform also has unique dicrotic notch, and its shape has been studied and shown to be related to arterial stiffness and aging [14]. To measure the deceleration and acceleration near the dicrotic notch, the first and second derivatives of PPG were calculated through three-point central difference [15,16]. For each heart beat cycle, we also calculated PPG waveform moving speed and acceleration in both vertical and horizontal directions. The duration and amplitude change in this movement were derived as two features [17].

A simple way to reduce the amount of data transmission amount through the network is by using a lower sampling rate. For high-frequency data like waveforms, the downsampling approach could directly reduce the amount of data. Therefore, it could be used before using other advanced data compression methods. In this experiment, we used equally spaced sampling, i.e., 120-, 60-, 30-, 15-, 10-, 5-Hz sampling, with evenly spaced sample location. Those sampling rates correspond to 50%, 75%, 87.5%, 93.8%, 95.8%, and 97.9% reduction rates.

5.0 RESULTS

5.1 Sampling Comparison Analysis for Trend Data

For the first 1-hour trend data, the instantaneous data at the sampling time were compared to the median values in the corresponding windows from the baseline. The root mean square error (RMSE) was used to measure the difference. Table 2 summarizes the RMSEs and the corresponding sampled points for HR, NBPS, NBPM, NBPD, RESP, SpO2, TMP, and CO2, at sampling rates of 6 seconds, 30 seconds, 1 minute, 5 minutes, 10 minutes, 15 minutes, and 30 minutes per sample.

Figure 2 shows the RMSE estimated from different numbers of cases. It indicates that N=15,000 is sufficient for the estimation, since the RMSE estimated from the N=801 (orange curve) almost overlaps with the RMSE estimated from the N=15,000 (grey curve), while the RMSE estimated from the N=177 (blue curve) diverged at those low sampling rates.

7

Table 2. RMSE Calculations for Various VS Trend Data (N=15,000)

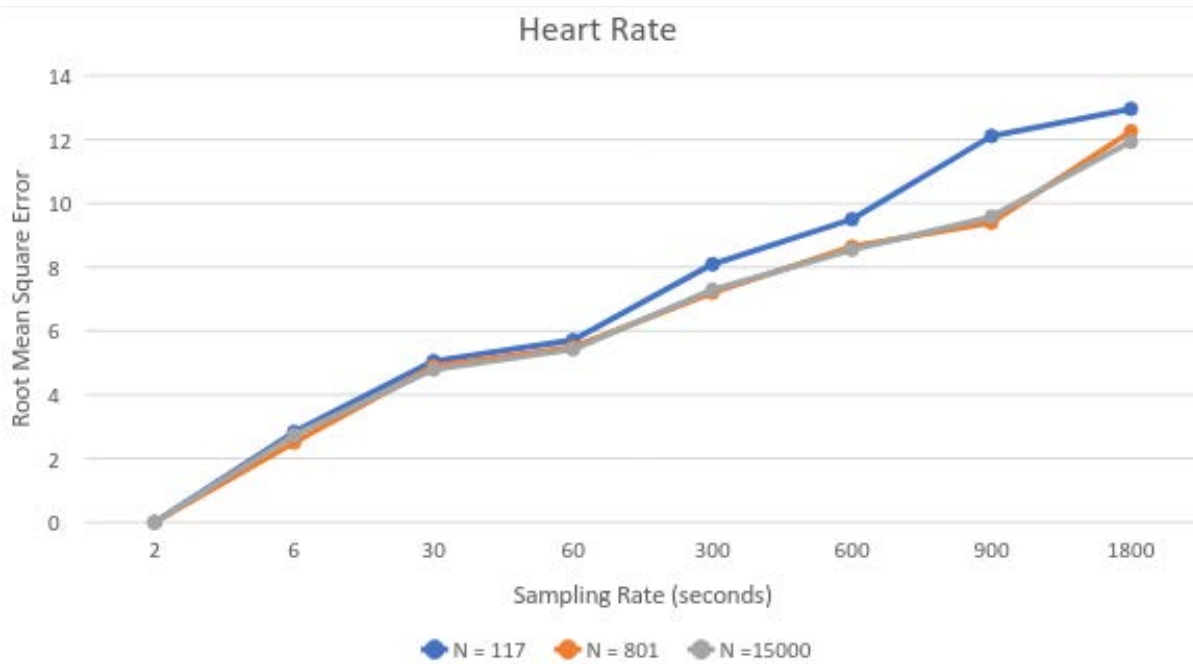| Sampling Rate ↓	HR: RMSE (samples)	NBPS: RMSE (samples)	NBPM: RMSE (samples)	NBPD: RMSE (samples)	RESP: RMSE (samples)	SpO2: RMSE (samples)	TMP: RMSE (samples)	CO2: RMSE (samples)
2 s [Baseline]	0.0 (24552031)	0.0 (23773062)	0.0 (23801398)	0.0 (23793745)	0.0 (22702691)	0.0 (24102090)	0.0 (95893)	0.0 (17352151)
6 s	2.7263 (8179574)	1.1906 (7917937)	0.8880 (7927408)	0.8618 (7925075)	4.7507 (7510147)	1.0442 (8026923)	0.1065 (31909)	0.7802 (5782117)
30 s	4.7922 (1630693)	3.1209 (1575301)	2.3485 (1577239)	2.2515 (1577274)	7.3212 (1455219)	1.8910 (1596678)	0.1730 (6318)	1.2970 (1155309)
1 min	5.4200 (812095)	4.4020 (782365)	3.3116 (783354)	3.1840 (783674)	7.6579 (703787)	2.1381 (793016)	0.2270 (3122)	1.6204 (576977)
5 min	7.2918 (165374)	9.2092 (161593)	6.9100 (161758)	6.5699 (161710)	9.4789 (154557)	3.0640 (162992)	1.0324 (670)	3.3370 (120393)
10 min	8.5490 (83457)	11.734 (82021)	8.7509 (82089)	8.3010 (82041)	10.154 (78297)	3.5906 (82357)	1.5049 (352)	4.6289 (62549)
15 min	9.5760 (56115)	13.278 (55330)	10.063 (55366)	9.5105 (55334)	10.649 (52816)	3.9769 (55402)	1.5853 (246)	5.4830 (43279)
30 min	11.925 (28863)	16.702 (28630)	12.733 (28634)	12.016 (28597)	12.006 (27381)	4.9370 (28467)	2.3287 (140)	7.1973 (24052)

Figure 2. RMSE calculations for HR for three values of case numbers (N=117, 801, and 15,000).

Next, we focused solely on HR data. We defined a tolerance as ±X beats per minute (bpm) or ±X% bpm, whichever is greater (where X = 1, 2, 3, 4, 5, 10, and 20). If the median value was within the bounds of the single-sampled value, we considered the median value to be an acceptable representation of the window. The windows column displays the total number of points compared in N=15,000 samples. This matrix allows us to select a tolerance and sampling rate given an error rate. Table 3 summarizes the percentages of data points that were within the X bpm or X% bpm differences compared with the baseline data.

8

Table 3. Percent HR within Bounds for N=15,000 (or HR Percent Accuracy for N=15,000)

Sampling Rate ↓	# Windows	±1 bpm or ±1% bpm (%)	±2 bpm or ±1% bpm (%)	±3 bpm or ±3% bpm (%)	±4 bpm or ±4% bpm (%)	±5 bpm or ±5% bpm (%)	±10 bpm or ±10% bpm (%)	±20 bpm or ±20% bpm (%)
2 s [Baseline]	24552031	100.00	100.00	100.00	100.00	100.00	100.00	100.00
6 s	8179574	74.43	85.42	90.98	94.06	95.91	99.04	99.88
30 s	812095	50.09	65.83	75.89	82.56	87.12	96.47	99.49
1 min	234615	42.55	59.31	70.51	78.27	83.70	95.24	99.24
5 min	165374	32.95	48.83	60.46	69.31	75.93	**91.74**	98.40
10 min	83457	28.33	43.17	54.93	63.96	71.00	88.99	97.63
15 min	56115	25.47	39.21	50.35	59.25	66.55	86.41	96.35
30 min	28863	19.63	31.19	41.38	49.92	57.15	79.73	94.74

The following graph (Figure 3) is another representation of the matrix above. Percent error was calculated by subtracting the percent accuracy from 100%. With a defined error percentage, we can select a sampling rate for different tolerances. For example, if we accept a 25% error rate, we can sample HR every 6 seconds with a tolerance of ±1 bpm or ±1% bpm or sample HR every 5 minutes with a tolerance of ±5 bpm or ±5% bpm.

Figure 4 helps visualize percentages of HR samples within preset bounds. The bounds for this figure are ±10 or 10%, indicated by the black curves (left figure) and white curves (right figure). The left scatter plot shows the instantaneous HR sampled every 5 minutes vs. the median HR within each 5-minute sampling window. The right figure uses a heat map where the density is in a logarithmic scale, showing that most data points (91.74%) are clustered within the defined bounds.
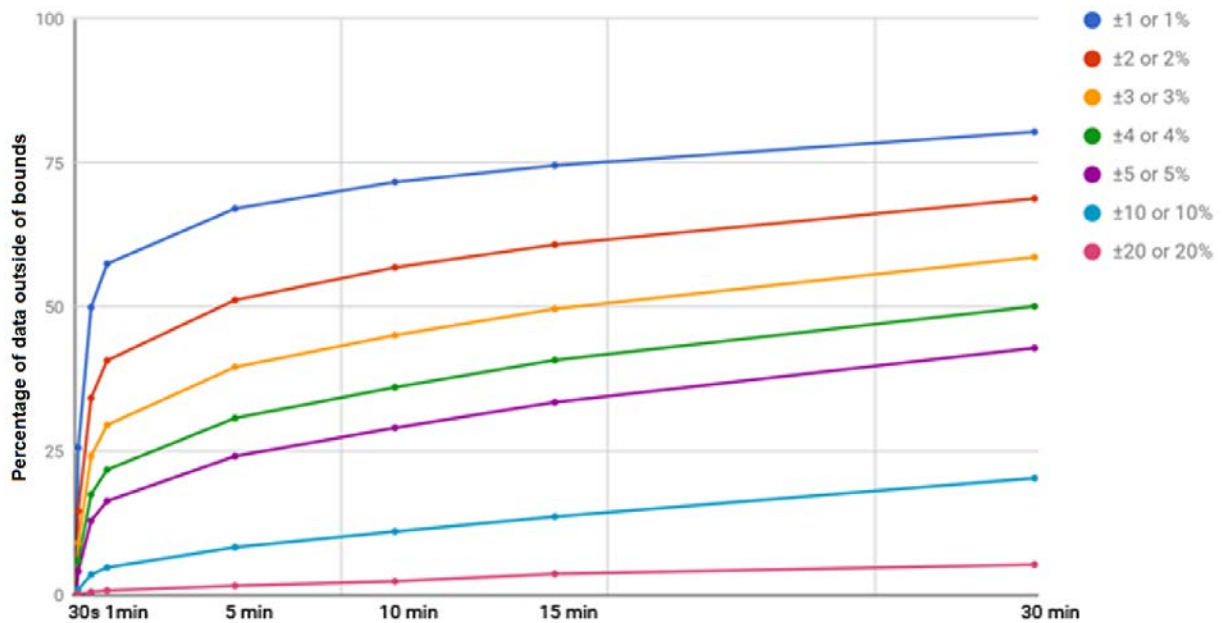

Figure 3. Percentages of data points outside of 1, 2, 3, 4, 5, 10, and 20 bps or % bps of the baseline at 6 s, 30 s, 1 min, 5 min, 10 min, 15 min, and 30 min.
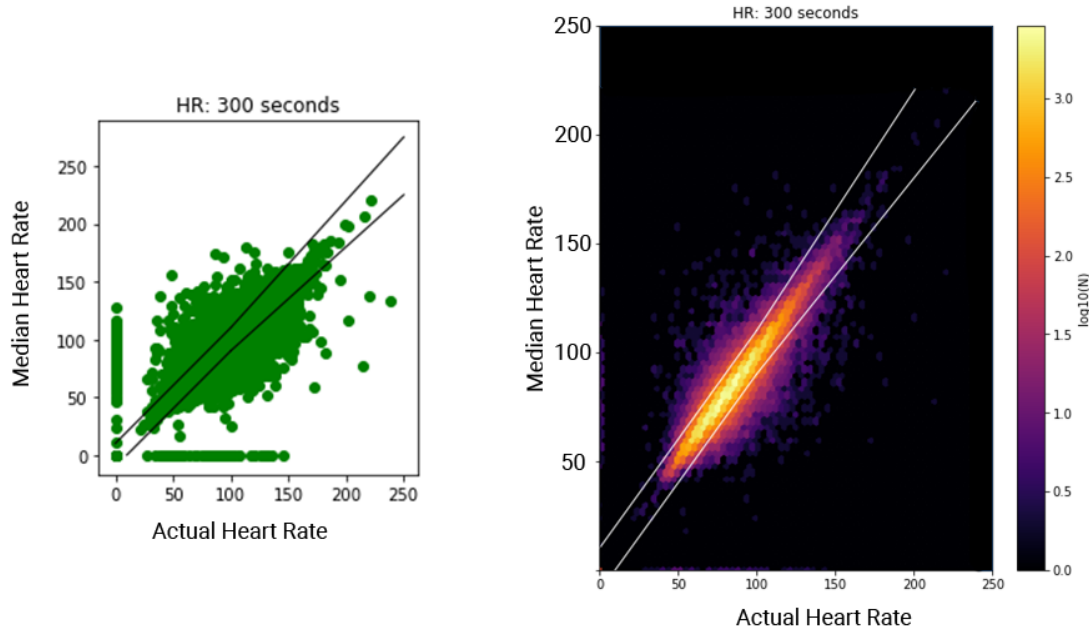
9

Figure 4. Scatter plot (left) of instantaneous HR sampled every 5 min vs. the median HR calculated from the corresponding windows with bounds as ±10 bps or ±10%; illustration of the density of data points (right).

5.2 Waveform Analysis

In the experiments of studying the effect of waveform sampling rates, we first compared the key variable, the mean R-R distance, calculated from ECG and PPG signals. For easy interpretation, we converted the mean R-R distance to HR. Figure 5 shows the mean, quartiles, minimum, and maximum of mean and standard deviation (SD) HR derived from ECG signals. The mean HR values were close when the sampling rates were above 60 Hz. The right panel shows the corresponding SD of HR. It can be observed that the variation of HR has been reduced with a lower sampling rate. Mean and SD HR calculations could sustain an even lower downsampling rate for PPG signal (Figure 6).

Second, we used all HRV variables derived from ECG or PPG signals as inputs of prediction models. Outcomes include UnX, MT, CAT (Figures 7 and 8), mortality, and LOS (Figures 9 and 10). It can be observed that variables calculated from ECG had a quicker performance drop with lower sampling rates, while variables calculated from PPG signal had a slower performance drop before the sampling rate went below 60 Hz.

The above experiments demonstrated the effect of downsampling on the key features and some prediction models. The waveform, such as ECG and PPG, contains abundant information on patients' physiologic condition. Feature extraction is one of the major uses of the waveform as input to certain models. The simulated downsampling rates allow us to search for a balance between compression rate and acceptable model performance.
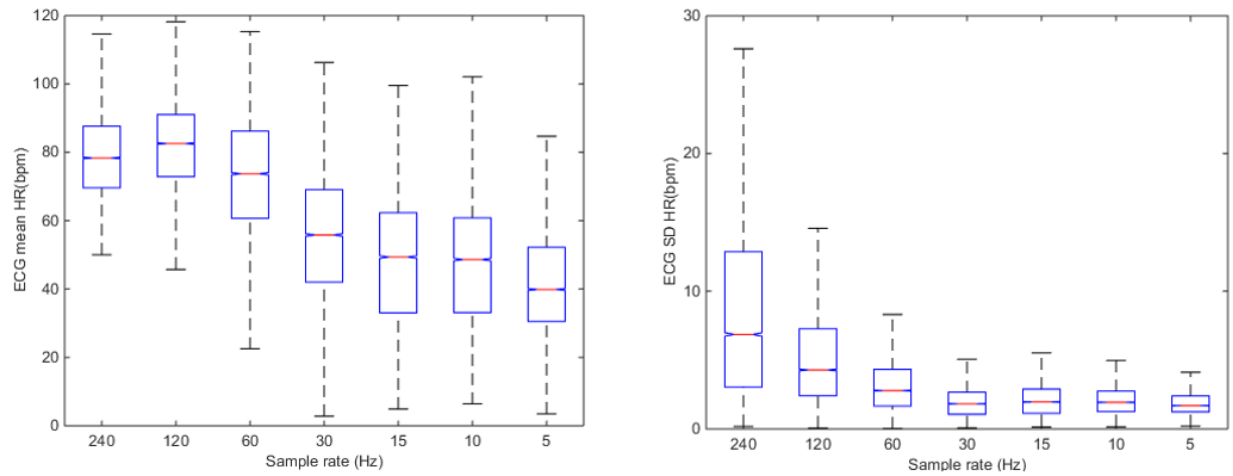
10

Figure 5. Boxplot of mean HR and SD of HR derived from ECG signal using various sampling rates.
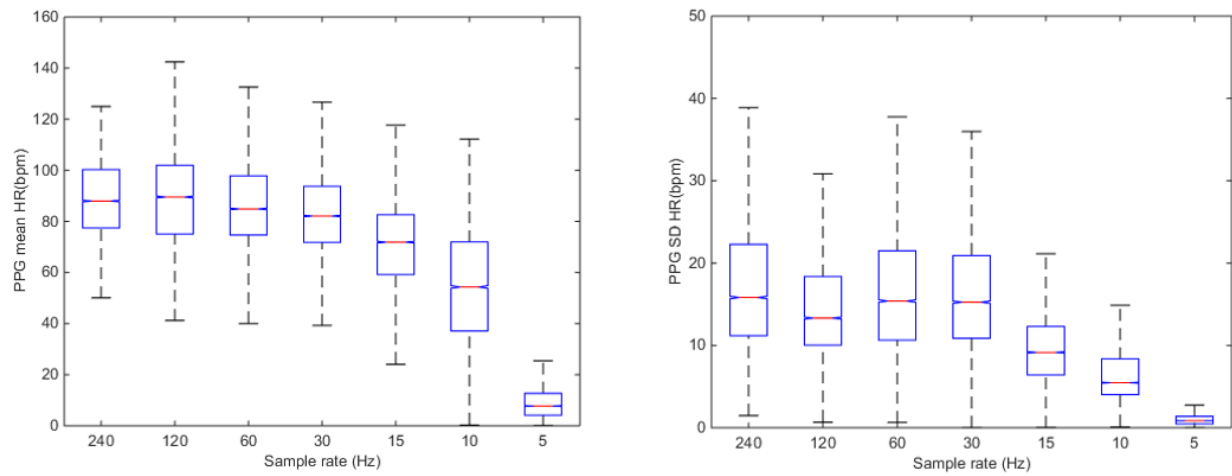

Figure 6. Boxplot of mean HR and SD of HR derived from PPG signal using various sampling rates.

11

Figure 7. AUROCs and 95% confidence interval (CI) in predicting UnX, MT, and CAT using ECG with sampling rates of 240, 120, 60, 30, 15, 10, and 5 Hz.

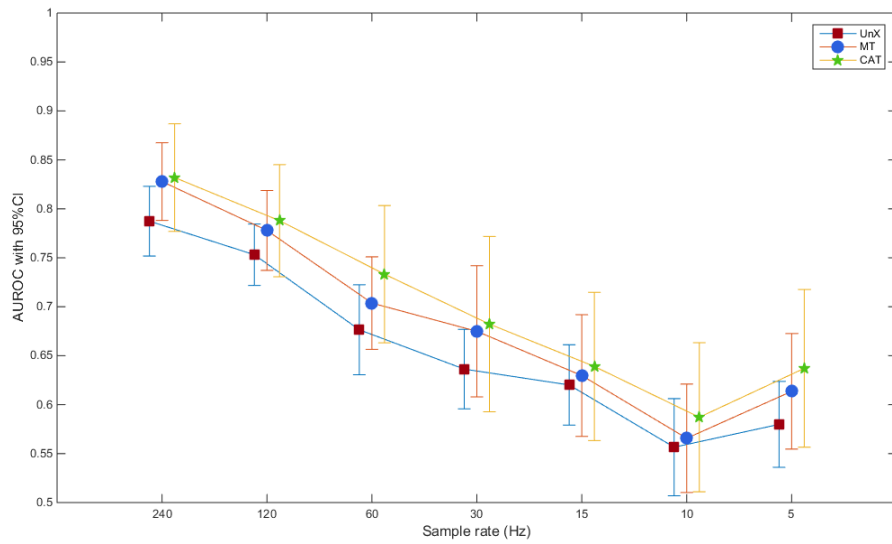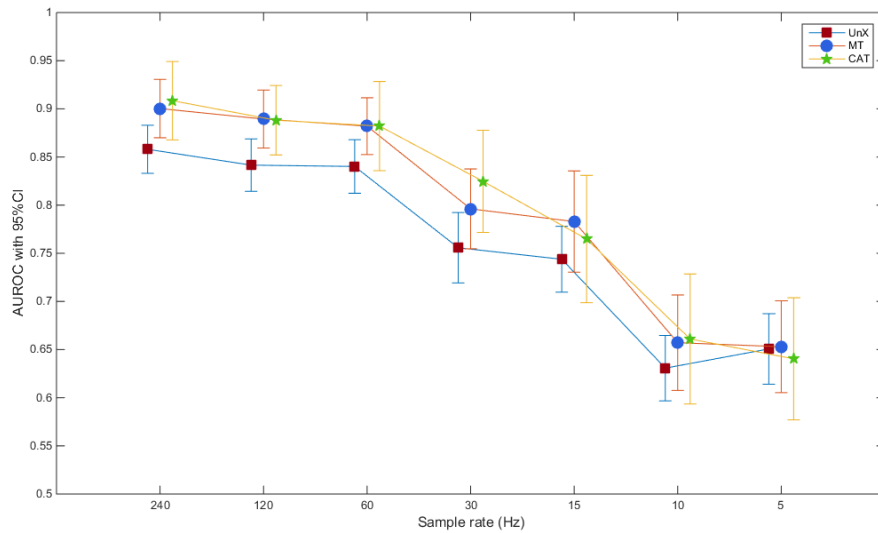**Figure 8. AUROCs and 95% CI in predicting UnX, MT, and CAT using PPG with sampling rates of 240, 60, 30, 15, 10, and 5 Hz.**
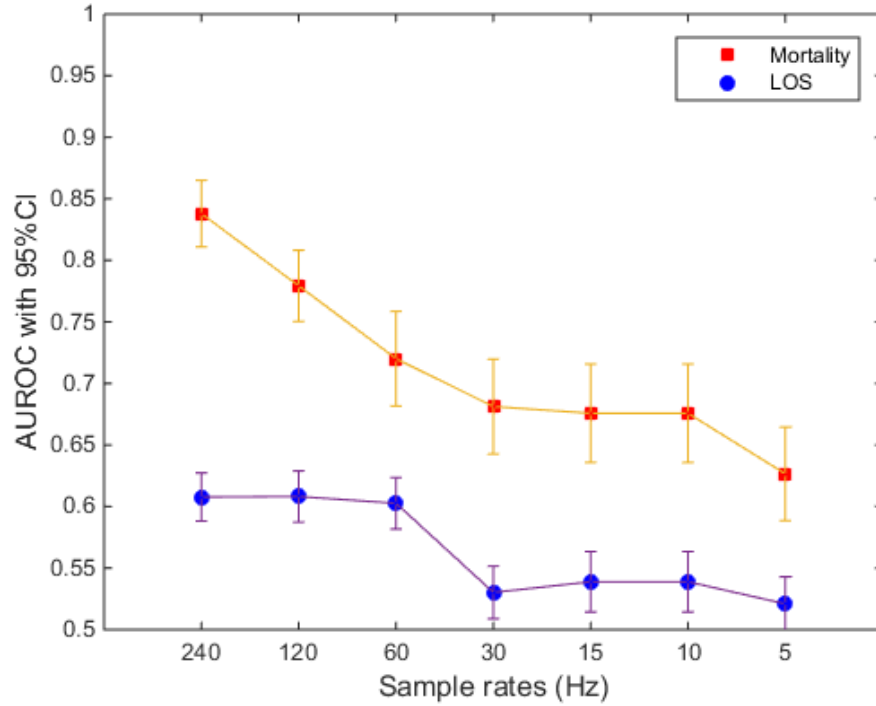
Figure 9. AUROCs and 95% CI in predicting mortality and LOS using ECG with sampling rates of 240, 120, 60, 30, 15, 10, and 5 Hz.
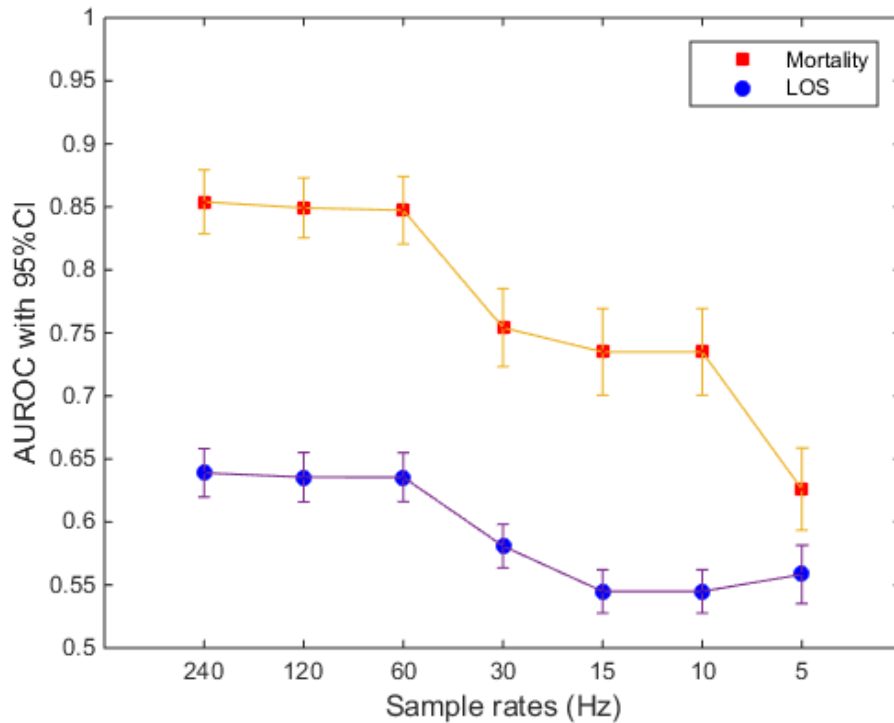

Figure 10. AUROCs and 95% CI in predicting mortality and LOS using PPG with sampling rates of 240, 120, 60, 30, 15, 10, and 5 Hz.

13

6.0 DISCUSSION

Modern communication technologies could gather remote information and transmit it to locations where complex analysis could be conducted. In austere environments, such as battlefield or natural disaster scenes, it is extremely difficult to deploy sufficient experienced health providers. Telemedicine with reliable and sufficient bandwidth could better serve the purpose of saving lives. However, networks in such environments are often unreliable with limited bandwidth. It is possible to use data compression methods to reduce the transmission amount. That said, with carefully identified important information, such as the variables that are useful for clinicians' decision making, the compression methods can be directly applied to the small set of selected data for further compactness. Therefore, it is necessary to use a large-scale real medical dataset and derive the related domain knowledge. In this study, we used data from 15,000 trauma patients, including high-fidelity waveforms (240 Hz), to develop evaluation matrices for selecting optimal VS sampling rates under limited transmission bandwidth. The statistical attributes of VS were calculated and compared for various downsampling rates. Such comparison provides guidance for sampling given the bandwidth in real conditions. Furthermore, high-fidelity waveforms were evaluated through a set of prediction models. The waveforms capture more internal physiologic pattern changes and are used in many predictive models. In this study, we found that very high sampling rates may not be necessary for calculating some variables in prediction models. For example, in predicting blood transfusion, ECG sampled at 120 Hz had less than a 5% reduction of AUROC compared to ECG sampled at 240 Hz. PPG signal is even more sustainable to lower sampling rate than ECG. Predicting the same outcomes, PPG sampled at 60 Hz had less than a 5% reduction of AUROC compared to PPG sampled at 240 Hz. These results indicate that it is possible to do downsampling before compression if required by the bandwidth limitation.

In this study, we only focused on the accuracy of the key VS variables and their performance changes under different downsampling rates. In reality, clinicians are also faced with other challenges such as data transmission error or loss due to the hostile environment. Theoretical development in compressive sensing has suggested that it is possible to reconstruct signals from an underdetermined set of measurements (very sparse samples), given that the signals are sparse and the measurement matrix satisfies certain conditions [18-21]. Most medical waveform signals possess certain internal structures that make them sparsely representable in some basis. For example, many signals can be represented with a few non-zeros in frequency domain, using a Fourier or wavelet basis. Such medical waveform sparsity allows us to tackle the above challenges. However, as a unique application, transmitting clinical waveforms in unreliable and limited-bandwidth networks has not been studied. The selection of sparsity representation domain and the measurement matrices have not been analyzed yet. The accuracy of the recovering algorithms also needs to be evaluated against real data collected from similar environments, such as prehospital and in-hospital early stages of resuscitation.

With the foundation established in this study, future research on recovering waveform signals from sparse samples could enhance the use of non-invasive and non-expensive medical sensor applications for high-fidelity data collection and transmission within an unreliable network with limited bandwidth. The ability to transmit medical waveform data will enable the use of more advanced diagnosis and decision making assistant tools and models in hostile environments where experienced clinicians are often not available. Hence, it is necessary to investigate techniques that could strengthen the capabilities of telemedical care in saving

patients' lives and improving their life quality by more accurate and rapid diagnosis based on faithful and rich physiologic information communicated from the remote field to the established health care facilities.

7.0 CONCLUSIONS

For efficient telemedical data transmission, a comprehensive evaluation of trade-off between data accuracy and communication network resources could guide optimal selection of data sampling rate and estimation of data reliability as well as their impact on clinical decisions. Identifying optimal sampling rates for high-fidelity waveforms could both reduce data transmission amount and enable wider use of waveforms for advanced diagnosis in predictive models.

This study shows it is possible to only compress a subset of observations for transmission. The amount of data could be further reduced if we identify variables that are essential to diagnosis and decision making.

8.0 REFERENCES

1. DuBoss JJ, Barmparas G, Inaba K, Stein DM, Scalea T, et al. Isolated severe traumatic brain injuries sustained during combat operations: demographics, mortality outcomes, and lessons to be learned from contrasts to civilian counterparts. J Trauma. 2011; 70(1):11-16.
2. Palmer RW. Integrated diagnostic and treatment devices for enroute critical care of patients within theater. In: Use of advanced technologies and new procedures in medical field operations. Proceedings of the RTO Human Factors and Medicine Panel (HFM) Symposium; 2010 Apr 19-21; Essen, Germany. Neuilly-sur-Seine, France: NATO Research and Technology Organisation; 2010. RTO-MP-HFM-182.
3. Provost F, Fawcett T. Data science and its relationship to big data and data-driven decision making. Big Data. 2013; 1(1):51-59.
4. Liu NT, Holcomb JB, Wade CE, Darrah MI, Salinas J. Utility of vital signs, heart rate variability and complexity, and machine learning for identifying the need for lifesaving interventions in trauma patients. Shock. 2014; 42(2):108-114.
5. Ernst G. Heart rate variability. London (UK): Springer; 2014:233-242.
6. Rajendra Acharya U, Paul Joseph K, Kannathal M, Lim CM, Suri JS. Heart rate variability: a review. Med Biol Eng Comput. 2006; 44(12):1031-1051.
7. Goodman B, Vargas B, Dodick D. Autonomic nervous system dysfunction in concussion (P01.265). Neurology. 2013; 80(7 Supplement):P01.265.
8. Heart rate variability standards of measurement, physiological interpretation, and clinical use. Task Force of the European Society of Cardiology and the North American Society of Pacing and Electrophysiology. Eur Heart J. 1996; 17(3):354-381.
9. Aslanidis T. Perspectives of autonomic nervous system perioperative monitoring—focus on selected tools. Int Arch Med. 2015; 8(22):1-9.
10. Mackenzie CF, Wang Y, Hu PF, Chen SY, Chen HH, et al. Automated prediction of early blood transfusion and mortality in trauma patients. J Trauma Acute Care Surg. 2014; 76(6):1379-1385.
11. Excel Medical Electronics, LLC. BedMasterEx operator's manual. Jupiter (FL): Excel Medical Electronics, LLC; 2013.

12. Pan J, Tompkins WJ. A real-time QRS detection algorithm. IEEE Trans Biomed Eng. 1985; 32(3):230-236.
13. Press WH, Teukolsky SA, Vetterling WT, Flannery BP. Statistical description of data. In: Numerical recipes: the art of scientific computing, 3rd ed. New York (NY): Cambridge University Press; 2007:720-772.
14. Voss A, Schroeder R, Heitmann A, Peters A, Perz S. Short-term heart rate variability—influence of gender and age in healthy subjects. PloS One. 2015; 10(3):e0118308.
15. Yousef Q, Reaz MB, Ali MA. The analysis of PPG morphology: investigating the effects of aging on arterial compliance. Measurement Science Review. 2012; 12(6):266-271.
16. Elgendi M, Norton I, Brearley M, Abbott D, Schuurmans D. Detection of a and b waves in the acceleration photoplethysmogram. Biomed Eng Online. 2014; 13:139.
17. Nitzan M, Babchenko A, Khanokh B, Landau D. The variability of the photoplethysmographic signal—a potential method for the evaluation of the autonomic nervous system. Physiol Meas. 1998; 19(1):93-102.
18. Candès EJ, Recht B. Exact matrix completion via convex optimization. Found Comput Math. 2009; 9(6):717-772.
19. Candès EJ, Tao T. The power of convex relaxation: near-optimal matrix completion. IEEE Trans Inf Theory. 2010; 56(5):2053-2080.
20. Coluccia G, Kuiteing SK, Abrardo A, Barni M, Magli E. Progressive compressed sensing and reconstruction of multidimensional signals using hybrid transform/prediction sparsity model. IEEE Journal on Emerging and Selected Topics in Circuits and Systems. 2012; 2(3):340-352.
21. Rubinstein R, Bruckstein AM, Elad M. Dictionaries for sparse representation modeling. Proceedings of the IEEE. 2010; 98(6):1045-1057.

LIST OF ABBREVIATIONS AND ACRONYMS

AUROC   area under the receiver operating characteristic curve

bpm   beats per minute

CAT   critical administrative threshold

CI   confidence interval

CO2   carbon dioxide

ECG   electrocardiogram

HR   heart rate

HRV   heart rate variability

LOS   length of stay

LSI   life-saving intervention

MT   massive transfusion

NBPD   non-invasive blood pressure / diastolic

NBPM   non-invasive blood pressure / mean

NBPS   non-invasive blood pressure / systolic

PPG   photoplethysmography

RESP   respiratory rate

RMSE   root mean square error

SD   standard deviation

SpO2   oxygen saturation

TBI   traumatic brain injury

TMP   temperature

TRU   trauma resuscitation unit

UnX   uncrossmatched blood

VS   vital sign